Optimization of Spatial Aperture-Sampled Mode Multiplexer for a Three-Mode Fiber

Miri Blau and Dan M. Marom, *Senior Member, IEEE*

***Abstract*— An optimization procedure for spatial mode multiplexing from individual single-mode fibers into a three-mode fiber based on a spatial aperture sampling concept has been developed. By placing space-variant imaging elements between the single-mode and few-mode fibers, each beam aperture can be shaped for lower loss coupling and low mode-dependent losses. The optimization achieves a record theoretical −1.5-dB insertion loss, improving on the previous theoretical −2-dB record.**

***Index Terms*— Few mode fibers (FMFs), mode-division multiplexing (MDM), optical communication.**

I. Introduction

SPACE-DIVISION multiplexing [1] has been attracting great attention in the last couple years, as a means to overcome the exhaustion of single mode fiber (SMF) transmission capacity [2]–[7]. The spatial degree of freedom can be exploited by transmitting over a set of different SMF, over multi-core fiber, or over different modes of a few-mode fiber (FMF). The FMF approach advantageously provides a capacity boost without a fiber count increase and only one physical port has to be managed. There are several technological barriers before mode-division multiplexing (MDM) can be adopted, one of which is the efficient multiplexing into, and demultiplexing out of, a FMF.

MDM is conventionally based on mode conversion manipulations and passive splitting or combining. In the *mode-conversion multiplexer* approach, phase masks (using etched phase plates [2], [7] or phase spatial light modulators [4], [6]) in the beam paths map each multiplexed mode to a separate demultiplexed SMF (and vice versa). Had there been no mode mixing throughout transmission, an information channel originating from a SMF, converted to a specific mode on a FMF with a mode conversion multiplexer, transported through the optical network and reconverted back to an output SMF by a mode conversion demultiplexer after transmission, would have remained pristine (apart for possible chromatic dispersion distortion) and amenable for detection (either direct or coherent). In practice, mode mixing throughout the transmission fiber results in distributed information mixing among the propagating modes, necessitating the use of multiple input, multiple output (MIMO) processing to unravel the original information channels.

Manuscript received July 25, 2012; revised August 29, 2012; accepted September 15, 2012. Date of publication September 28, 2012; date of current version November 20, 2012.

The authors are with the Department of Applied Physics, Hebrew University, Jerusalem 91904, Israel (e-mail: miri.blau10@gmail.com; danmarom@cc.huji.ac.il).

Color versions of one or more of the figures in this letter are available online at http://ieeexplore.ieee.org.

Digital Object Identifier 10.1109/LPT.2012.2220536

Thus, the main advantage of the mode conversion multiplexer, which attempts to map each spatial mode of the FMF to a separated mode of a SMF, is rarely utilized and the MIMO processing overhead is incurred. Moreover, beam conversion multiplexers are associated with inherently high insertion loss (IL) metrics, due to additional passive combining/splitting losses.

An alternative, *spatial aperture-sampling mode demultiplexer*, eliminates the need for a splitter/combiner and its associated losses. The basic concept of this demultiplexer is the sampling of the FMF aperture instead of the conversion of each mode. One arrangement for this demultiplexer utilizes adiabatic tapering down of a SMF bundle to match the FMF aperture [8]. Alternatively, the individual apertures can be abruptly coupled to the FMF by free-space imaging or direct contact. The imaging approach has been recently demonstrated for a three mode fiber [9]. The individual beams of the multiple input SMF sources are imaged onto distinct locations within the FMF core. Each SMF image serves as an independent source and illuminates a finite aperture of the fiber face, hence it will couple with fixed efficiency to each linearly polarized (LP) mode of the FMF (see Fig. 1). The direct contact approach has also been suggested [10], and analyzed as a matrix operation, mapping the individual mode amplitudes onto the distinct fiber modes with fixed efficiency. As the excitation distribution of the modes at the spatial aperture-sampling mode multiplexer is fixed, the information can still be recovered by MIMO processing [10]. In other words, since MIMO processing is required for handling mode mixing in transmission in any event, then additional FMF ingress mode-mixing due to the spatial aperture-sampling multiplexer (and FMF egress mixing) do not add complexity to the MIMO processing, which now is also tasked with recovering the coupling matrix elements (which can also be deterministically provided).

In this letter we expand the spatial aperture-sampling concept by introducing optimized aperture distributions. All previous works considered circular Gaussian field distributions, a close match to the SMF fundamental mode. We demonstrate that by placing space variant imaging elements between the SMF and the FMF, we can theoretically reduce the IL from −2 dB (circular Gaussian case) down to below −1.5 dB, while keeping mode dependent losses (MDL) below 0.2 dB.

II. Spatial Sampling Multiplexer Optimization

Following ref. 10, let the FMF support N propagating modes, where the ith mode has a transverse normalized field distribution of $\psi_i(x, y)$. These modes are known to be

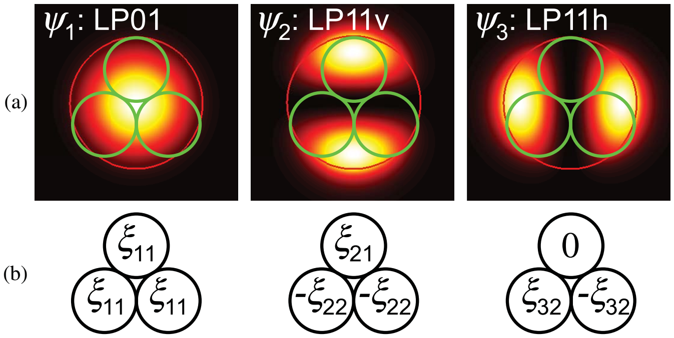

Fig. 1. (a) LP modes of a three-mode fiber. Core outlined in red, and three circular apertures in green. (b) ξ_{ik}, coupling coefficient values, defined as a coupling integral between the jth mode and the kth finite aperture beam; coupling values illustrated here from the symmetries and anti-symmetries of the three modes.

orthogonal. Next, consider a projection operation, defined as a coupling integral between each mode and a finite aperture beam,

$$\int \psi_i \cdot \varphi_k^* \, dA = \xi_{ik} \tag{1}$$

where φ_k(x,y) is the normalized beam field distribution, defined over a finite, non-overlapping region of the FMF aperture. These beams are orthogonal to each other, due to the latter property.

The choice of apertures has to satisfy a few key requirements for multiplexing and demultiplexing: a) The number of apertures should match the number of modes, to match basis set size, b) the total power transfer efficiency from mode ψ_i onto aperture beams (demux) should be high, $\Sigma\, |\xi_{ik}|^2$, c) the differences between total power transfer efficiencies per mode should be minimized, for low mode dependent loss (MDL), and d) the projection operation should maintain mode orthogonality,

$$\langle \xi_{i1}, \xi_{i2}, \xi_{i3} \rangle \cdot \langle \xi_{j1}, \xi_{j2}, \xi_{j3} \rangle^* = 0 \tag{2}$$

for $i \neq j$. We can now construct an $N \times N$ matrix, ξ, whose elements ξ_{ik} are the coupling coefficients from the ith mode into the kth aperture. The matrix ξ transforms an N-dimensional vector of the modal content ψ to an N-dimensional vector of the finite aperture beam φ (demultiplexer). Its Hermitian conjugate, $\xi^\dagger$, transforms back from the vector φ to fiber modes ψ. If we satisfy the orthogonality condition (Eq. (2)), it is easy to show that $\xi\xi^\dagger$ is a diagonal matrix. Its trace elements are smaller than one due to losses in the transformation (i.e. the transformation is not unitary), and the trace element differences contribute to MDL, which lead to capacity loss [11].

The procedure for selecting the optimized beam distribution consists of selecting well-behaving apertures (ones that can be synthesized by spatial beam shaping techniques), varying the degrees of freedom associated with each selected aperture form, calculating the coefficient matrix ξ, screening out the variations whose MDL is above an acceptable threshold (e.g., 0.3 dB), and then selecting the realization with the lowest IL. Apertures obeying a 120° azimuthal symmetry will satisfy the orthogonality criterion, by symmetry.

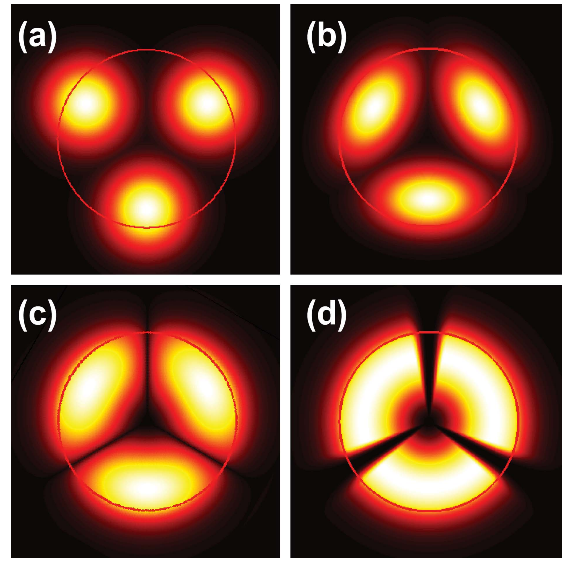

Fig. 2. Optical apertures optimally subtending the three-mode fiber core. (a) Circular Gaussian apertures, (b) elliptical Gaussian apertures with 0.79 eccentricity, radial Bessel with (c) azimuthal cosine raised to 0.3 power, and (d) adjustable Raised cosine function with $\beta = 0.785$.

The simplest apertures to consider are circular Gaussian beams (Fig. 2a), which can be implemented by imaging the three SMF modes onto the FMF. The beam diameter and radial distance are the only parameters to vary. Optimization yields the coupling coefficient matrix

$$\xi = \begin{bmatrix} 0.466 & 0.653 & 0 \\ 0.466 & -0.328 & 0.567 \\ 0.466 & -0.328 & -0.567 \end{bmatrix} \Rightarrow \begin{array}{c} \overline{\text{IL}} = -1.90 \text{ dB} \\ \text{MDL} = 0.07 \text{ dB}. \end{array}$$

The LP01 mode equally excites all three apertures, the LP11h results in one nulled aperture due to symmetry and an equal division of the energy between the two other apertures. In the LP11v case it is clear that a sufficient condition to ensure orthogonality according to Eq. (2) is $|\xi_{21}| = 2|\xi_{22}|$. The calculated coefficient values are consistent with the anticipated relationships, as shown Fig. 1.

The more generalized form of elliptical Gaussian beams, introduces an ellipse eccentricity optimization parameter (Fig. 2b) resulting in the coupling coefficient matrix:

$$\xi = \begin{bmatrix} 0.475 & 0.667 & 0 \\ 0.475 & -0.335 & 0.582 \\ 0.475 & -0.335 & -0.582 \end{bmatrix} \Rightarrow \begin{array}{c} \overline{\text{IL}} = -1.7 \text{ dB} \\ \text{MDL} = 0.05 \text{ dB}. \end{array}$$

While the aperture coupling coefficients are quite similar, the coupling efficiency of elliptical Gaussian peaks at an eccentricity value of 0.78. Obtaining an elliptical beam is rather simple with anamorphic imaging elements.

More complex apertures can be obtained by creating beams that are defined by separable functions (in radial, $R(r)$, and azimuthal, $\Theta(\theta)$, directions). We considered several radial dependencies, such as Gaussian and super-Gaussian of variable width and radial distance. However, the functional form that provided the best results was of Bessel dependence, similar to the radial form of the LP11 modes [12], namely

$$R(r) = \begin{cases} J_1\left(\frac{\kappa a}{r}\right) & r \le a \\ \frac{J_1(\kappa)}{K_1(\gamma)} \cdot K_1\left(\frac{\gamma a}{r}\right) & r > a. \end{cases} \quad (3)$$

When κ and γ are defined the same way as in the LP11 mode [12] where the core radius parameter, a, was a variable screened for best performance (not linked to physical core radius of fiber). In the azimuthal direction, two forms were considered; one was a cosine scaled to span over $\pm\pi/3$ and raised to a variable power, such that

$$\Theta(\theta) = \cos^x\left(\frac{3\varphi}{2}\right). \quad (4)$$

Best performance metrics were obtained for $x \cong 0.3$, with a coupling coefficient matrix of:

$$\xi = \begin{bmatrix} 0.494 & 0.685 & 0 \\ 0.494 & -0.343 & 0.593 \\ 0.494 & -0.343 & -0.593 \end{bmatrix} \Rightarrow \begin{matrix} \overline{\text{IL}} = -1.46 \text{ dB} \\ \text{MDL} = 0.17 \text{ dB}. \end{matrix}$$

An alternative azimuthal dependence of a raised cosine was attempted, with its endpoints fixed at $\pm\pi/3$ and a transition width parameterized by $\beta \in \langle 0, 1\rangle$, according to

$$\Theta(\theta) = \begin{cases} 1 & |\varphi| \le \beta\pi/3 \\ 0.5\left[1 + \cos\left(\frac{3}{1-\beta}\left(|\varphi| - \frac{\beta\pi}{3}\right)\right)\right] & \beta\pi/3 < |\varphi| \le \pi/3. \end{cases} \quad (5)$$

When optimizing with the raised cosine azimuthal dependence, the fractional transition distance converges onto zero when minimizing the IL only (or $\beta \to 1$ and the angular dependence becomes rectangular), reaching an average IL value of -1.46 dB (identical to the cosine raised to a power of 0.3 case) but with elevated MDL value of 0.61 dB. The resulting apertures appear as a ring split to three equal angular segments (see Fig. 3). However, the apertures have an abrupt transition which is not realizable experimentally. Two other values of interest for the β parameter are at 0.55 (shown in Fig. 3 at center), where we get an IL of -1.8 dB and zero MDL, and at 0.785 (intensity distribution shown in Fig 2-(d)), where our MDL criterion of 0.3 dB is satisfied, resulting in a coefficient matrix of:

$$\xi = \begin{bmatrix} 0.491 & 0.672 & 0 \\ 0.491 & -0.336 & 0.583 \\ 0.491 & -0.336 & -0.583 \end{bmatrix} \Rightarrow \begin{matrix} \overline{\text{IL}} = -1.6 \text{ dB} \\ \text{MDL} = 0.3 \text{ dB} \end{matrix}$$

Generating the aperture shapes described by these separable functions is possible with the use of two phase-only diffractive optical elements (DOE) placed in cascade, where the first DOE controls the amplitude distribution at the plane of the second DOE via diffraction, and the latter adjusts the phase distribution to achieve efficient coupling into the FMF (as shown in Fig. 4). By employing phase-only DOE encoding, theoretically efficient diffraction efficiency may be achieved, reducing the additional insertion losses of the multiplexer to a minimum. The aperture functions are required to be smooth and continuous, allowing both DOEs to be encoded with slowly varying and moderate phase depths. Anti-reflection coating can further reduce the Fresnel reflections and achieve low loss attributes.

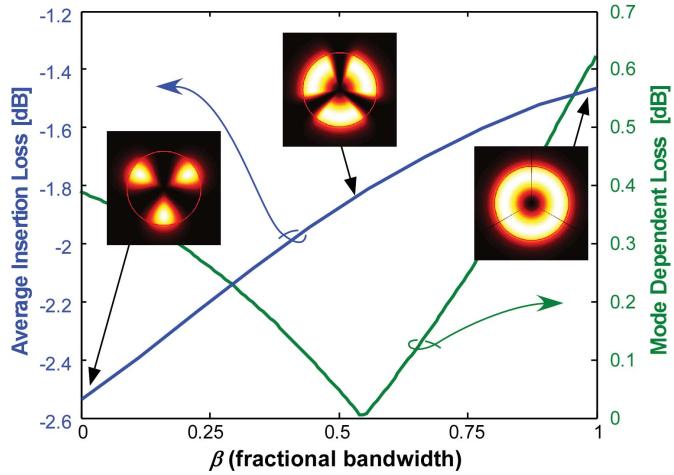

Fig. 3. Average insertion loss and mode-dependent loss for radial Bessel and azimuthal raised cosine functional dependence, for different transitional bandwidth.

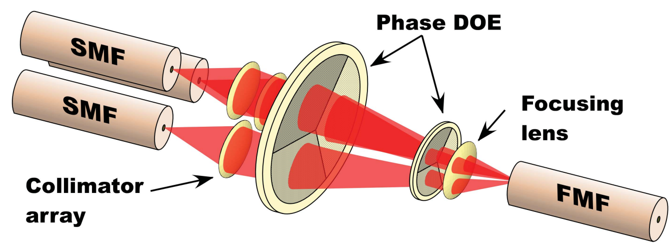

Fig. 4. General optical arrangement of aperture shaping for a spatial aperture-sampling mode demultiplexer. The separate SMFs beams are shaped by two space-variant, phase-only DOEs and then focused onto the FMF.

The mode coupling coefficients (Eq. 1) and the IL and MDL calculations performed herein left out the polarization degree of freedom. However, since the two polarization states are orthogonal in fiber modes and in the projection operation (which operates in the scalar regime), the technique extends independently over both polarization states. Note that the required projection operation can also be performed in three-dimensional guided waveguides, as being developed for chip to chip interconnect by photonic wire-bonds [13].

III. Conclusion

We have demonstrated how the performance of a spatial aperture-sampling mode multiplexer can be improved by optimizing the beam aperture distributions. This optimization demonstrated that multiplexing to a three-mode fiber can potentially reach a record insertion loss value of -1.5 dB and low MDL of 0.2 dB, achieved with an azimuthal cosine raised to 0.3 power. The spatial sampling approach can also be applied to FMF supporting higher mode counts, thus being scalable, as opposed to the mode conversion solution. All simulations were performed with LP modes obtained from analytic solutions to the step-index dielectric fiber (SMF radius of 4.4 microns, $\Delta n = 0.1$ ($V = 1.997$) and FMF radius of 6.5 microns, $\Delta n = 0.13$ ($V = 3.613$), where V is the normalized frequency). The technique can be adapted to support other refractive index distributions as well.

REFERENCES

[1] S. Berdagué and P. Facq, "Mode division multiplexing in optical fibers," *Appl. Opt.*, vol. 21, no. 11, pp. 1950–1955, 1982.

[2] R. Ryf, *et al.*, "Space-division multiplexing over 10 km of three-mode fiber using coherent 6 × 6 MIMO processing," in *Proc. OFC 2011*, pp. 1–3, paper PDPB10.

[3] S. Randel, *et al.*, "6×56-Gb/s mode-division multiplexed transmission over 33-km few-mode fiber enabled by 6×6 MIMO equalization," *Opt. Express*, vol. 19, no. 17, pp. 16697–16707, 2011.

[4] M. Salsi, *et al.*, "Transmission at 2×100 Gb/s, over two modes of 40 km-long prototype few-mode fiber, using LCOS based mode multiplexer and demultiplexer," in *Proc. OFC 2011*, pp. 1–3, paper PDPB9.

[5] A. Al Amin, A. Li, S. Chen, X. Chen, G. Gao, and W. Shieh, "Dual-LP_{11} mode 4×4 MIMO-OFDM transmission over a two-mode fiber," *Opt. Express*, vol. 19, no. 17, pp. 16672–16679, 2011.

[6] C. Koebele, *et al.*, "Two mode transmission at 2×100 Gb/s, over 40 km-long prototype few-mode fiber, using LCOS-based programmable mode multiplexer and demultiplexer," *Opt. Express*, vol. 19, no. 17, pp. 16593–16600, 2011.

[7] E. Ip, *et al.*, "88×3×112-Gb/s WDM transmission over 50 km of three-mode fiber with inline few-mode fiber amplifier," in *Proc. ECOC 2011*, pp. 1–2, paper Th.13.C.2.

[8] R. R. Thomson, T. A. Birks, S. G. Leon-Saval, A. K. Kar, and J. Bland-Hawthorn, "Ultrafast laser inscription of an integrated photonic lantern," *Opt. Express*, vol. 19, no. 6, pp. 5698–5705, 2011.

[9] R. Ryf, *et al.*, "Low-loss mode coupler for mode-multiplexed transmission in few-mode fiber," in *Proc. OFC 2012*, pp. 1–3, paper PDP5B.5.

[10] H. Bülow, "Optical mode demultiplexing by optical MIMO filtering of spatial samples," *IEEE Photon. Technol. Lett.*, vol. 24, no. 12, pp. 1045–1047, Jun. 15, 2012.

[11] A. Nafta, E. Meron, and M. Shtaif, "Capacity limitations in fiber-optic communication systems as a result of polarization-dependent loss," *Opt. Lett.*, vol. 34, no. 23, pp. 3613–3615, 2009.

[12] J. A. Buck, *Fundamentals of Optical Fibers*, 2nd ed. New York: Wiley, 1995.

[13] N. Lindenmann, *et al.*, "Photonic wire bonding: A novel concept for chip-scale interconnects," *Opt. Express*, vol. 20, no. 16, pp. 17667–17677, 2012.